Acta Histochemica 125 (2023) 151978

Contents lists available at ScienceDirect

Acta Histochemica

journal homepage: www.elsevier.com/locate/acthis

Taurine induces upregulation of p53 and Beclin1 and has antitumor effect in human nasopharyngeal carcinoma cells *in vitro* and *in vivo*

Motohiko Okano [a,b,1], Feng He [a,1], Ning Ma [c], Hatasu Kobayashi [a], Shinji Oikawa [a], Komei Nishimura [b], Isao Tawara [b,*], Mariko Murata [a,**]

[a] Department of Environmental and Molecular Medicine, Mie University Graduate School of Medicine, Tsu, Mie, Japan
[b] Department of Hematology and Oncology, Mie University Graduate School of Medicine, Tsu, Mie, Japan
[c] Graduate School of Health Science, Suzuka University of Medical Science, Suzuka, Mie, Japan

ARTICLE INFO

Keywords:
Taurine
Nasopharyngeal carcinoma
Antitumor
Apoptosis
Autophagy

ABSTRACT

Taurine is an amino acid that has several physiological functions. Previously, we reported the apoptosis-inducing effect of taurine in human nasopharyngeal carcinoma (NPC) cells *in vitro*. However, the effect of taurine on NPC cell growth *in vivo* has not been elucidated. Autophagy plays an important role in cell metabolism and exhibits antitumor effects under certain conditions. In this study, we investigated the effects of taurine on apoptosis- and autophagy-related molecules in NPC cells *in vitro* and *in vivo*. In our *in vitro* study, NPC cells (HK1-EBV) were treated with taurine, and Western blot and immunocytochemical analyses revealed that taurine co-upregulated Beclin 1 and p53, with autophagy upregulation. In the *in vivo* study, we used a nude mouse model with subcutaneous xenografts of HK1-EBV cells. Once the tumors reached 2–3 mm in diameter, the mice were provided with distilled water (control group) or taurine dissolved in distilled water (taurine-treated group) *ad libitum* (day 1) and sacrificed on day 13. The volume and weight of the tumors were significantly lower in the taurine-treated group. Using immunohistochemistry (IHC), we confirmed that taurine treatment reduced the distinct cancer nest areas. IHC analyses also revealed that taurine promoted apoptosis, as evidenced by an increase in cleaved caspase-3, accompanied by upregulation of p53. Additionally, taurine increased LC3B and Beclin 1 expression, which are typical autophagy markers. The present study demonstrated taurine-mediated tumor growth suppression. Therefore, taurine may be a novel preventive strategy for NPC.

1. Introduction

Nasopharyngeal carcinoma (NPC) is a distinct type of head and neck malignancy. Although NPC incidence in Western countries is only 0.4 cases per 100,000 people per year (Chen et al., 2019), it is markedly higher in the southern regions of China at 14–25 cases per 100,000 people per year (Chang et al., 2021). Radiotherapy and chemotherapy have improved the prognosis of NPC; however, the five-year overall survival rate of patients with advanced NPC remains at approximately 60 % (Chen et al., 2019; Leung et al., 2006). Therefore, novel preventive or therapeutic strategies for NPC are urgently required.

Taurine (2-aminoethane-sulfonic acid) is a sulfur-containing amino acid lacking a carboxyl group and is found in millimolar concentrations in most mammalian tissues (Schuller-Levis and Park, 2003). Although humans can synthesize taurine endogenously, they depend on their diet for taurine production (Yamori et al., 2010), which is mostly found in seafood. Taurine has several physiological functions, including antioxidation, antiinflammation, bile salt conjugation, osmoregulation,

Abbreviations: ERK, extracellular signal-related kinase 1 and 2; ICC, immunocytochemistry; IHC, immunohistochemistry; MAPK, mitogen-activated protein kinase; MELAS, mitochondrial myopathy, encephalopathy, lactic acidosis, and stroke-like episodes; MIF, macrophage migration inhibitory factor; mTORC1, mechanistic target of rapamycin protein kinase complex 1; NPC, nasopharyngeal carcinoma; p-, phospho-; PBS, phosphate buffered saline; PTEN, phosphatase and tensin homolog; TAUT, taurine transporter; TBST, Tris buffered saline containing 0.1 % (v/v) Tween-20; TFEB, transcription factor EB.

* Correspondence to: Department of Hematology and Oncology, Mie University Graduate School of Medicine, 2–174, Edobashi, Tsu, Mie 514-8507, Japan.
** Correspondence to: Department of Environmental and Molecular Medicine, Mie University Graduate School of Medicine, 2-174, Edobashi, Tsu, Mie 514-8507, Japan.
E-mail addresses: itawara@clin.medic.mie-u.ac.jp (I. Tawara), mmurata@med.mie-u.ac.jp (M. Murata).
[1] Equal contribution.

https://doi.org/10.1016/j.acthis.2022.151978
Received 26 September 2022; Received in revised form 22 November 2022; Accepted 22 November 2022
Available online 2 December 2022

membrane stabilization, cell volume regulation, and autophagy induction (Kim and Cha, 2014; Lambert, 2004; Lambert et al., 2008; Lang et al., 2003; Schuller-Levis and Park, 2003). Taurine has been reported to have anticancer effects in certain types of cancer cells by regulating apoptosis-related molecules (Surarak et al., 2021; Tu et al., 2018; Zhang et al., 2014), improving antiinflammation and antioxidant capacities (Kim et al., 2017; Ma et al., 2022; Wang et al., 2020), and regulating immunity (Ibrahim et al., 2018; Maher et al., 2005). We also previously reported the apoptosis-inducing effect of taurine in NPC cells *in vitro* by flow cytometry and upregulation of cleaved caspase-3 and -9 by Western blot analysis (He et al., 2018) and immunocytochemistry (ICC) (He et al., 2019). However, the effects of taurine on NPC cell growth *in vivo* have not yet been thoroughly elucidated.

Autophagy is a catabolic process by which cellular material is delivered to lysosomes for degradation, leading to basal turnover of cell components and providing energy and macromolecular precursors (Levy et al., 2017). Autophagy plays a pivotal role in the metabolism of both normal and cancerous cells. Additionally, Beclin 1, an autophagy-associated protein, functions as a tumor suppressor by regulating p53 levels (Liu et al., 2011). LC3B is a known marker for assessing autophagy. During autophagy, the cytosolic form of LC3B (LC3B-I) is conjugated to phosphatidylethanolamine to form LC3B-II, which localizes to the autophagosome (Kabeya et al., 2000). Although autophagy suppresses cancer growth in some contexts (Levy et al., 2017; Yue et al., 2003), its role in cancer, including NPC, remains unclear.

In this study, we found that taurine upregulated both Beclin 1 and p53 in NPC cells *in vitro*, and upregulated autophagy, as detected by Western blotting and ICC, as well as apoptosis, as previously reported (He et al., 2019). Subsequently, we investigated the effect of taurine on NPC tumor growth *in vivo* using a nude mouse model bearing NPC cell xenografts, and analyzed apoptosis- and autophagy-related molecules using an immunohistochemical (IHC) approach.

2. Materials and methods

2.1. Cell culture

The human NPC cell line (HK1-EBV) was a kind gift from Professor Sai-Wah Tsao (Hong Kong University) (Huang et al., 1980; Lo et al., 2006). The HK1-EBV cell line has been authenticated using short tandem repeat profiling within the last three years. The cells were cultured in RPMI 1640 medium (Thermo Fisher Scientific Inc., Waltham, MA, USA) supplemented with 10 % fetal bovine serum (Thermo Fisher Scientific Inc.), 100 U/ml penicillin, and 100 μg/ml streptomycin (Thermo Fisher Scientific Inc.) at 37 °C in a 5 % CO_2 incubator. Our previous study (He et al., 2018) showed that treatment with taurine at 32 mM for 48 h most effectively suppressed NPC cell proliferation *in vitro*. Therefore, we treated NPC cells *in vitro* under the same conditions.

2.2. Western blot analyses

After treatment with taurine, the cells were lysed using RIPA buffer (Cell Signaling Technology Inc., Danvers, MA, USA) supplemented with phenylmethylsulfonyl fluoride (Nacalai Tesque Inc.). Equal amounts of protein were separated by SDS-PAGE and transferred to polyvinylidene fluoride membranes (0.45 μm, Merck, Darmstadt, Germany). The membranes were blocked with Tris-buffered saline containing 0.1 % (v/v) Tween-20 (Nacalai Tesque Inc.) (TBST) and 5 % (w/v) skimmed milk (Becton Dickinson, Franklin Lakes, NJ, USA; cat. no. 232100), and incubated overnight at 4 °C with primary antibodies: Beclin 1 (rabbit IgG; Abcam plc, Cambridge, UK; cat. no. ab62557, 1:2000), p53 (mouse IgG2a, Merck; cat. no. OP43, 1:1000), LC3B (mouse IgG2b; Cell Signaling Technology Inc., cat. no. 83506s, 1:1000) and GAPDH (mouse IgG1, Santa Cruz Biotechnology, Inc., Dallas, TX, USA; cat. no., sc-47724, 1:3000). After washing with TBST, the membranes were incubated with horseradish peroxidase (HRP)-conjugated secondary antibodies (1:2000, Cell Signaling Technology Inc.; cat. no. 5127S, 7076S) for 1 h at 25 °C and finally developed using an electrochemiluminescence system (GE Healthcare, Little Chalfont, UK). Protein bands were detected using an AMERSHAM ImageQuant 800 (Cytiva, Tokyo, Japan), and band intensities of Western blots were quantitatively measured by calculating integrated grayscale densities in consistently sized windows incorporating each band using the ImageJ software (ver. 1.53e; National Institutes of Health, Bethesda, MD, USA). All experiments were performed in quadruplicate.

2.3. ICC analyses

Cells were harvested by trypsin, fixed on slides with 4 % (v/v) formaldehyde in phosphate-buffered saline (PBS) for 10 min at room temperature after treatment with taurine, and washed thrice with PBS. The cells were treated with 1 % (v/v) Triton X-100 (Nacalai Tesque Inc.) for 10 min and then incubated with 1 % (w/v) skim milk (Becton Dickinson) for 15 min at room temperature. ICC was performed by incubation with the following primary antibodies overnight at 25 °C: Beclin 1 (rabbit IgG, Abcam plc, cat. no. ab62557, 1:200), p53 (mouse IgG2a, Merck; cat. no. OP43, 1:200), and LC3B (mouse IgG2b; Cell Signaling Technology Inc., cat. no. 83506s, 1:200). After washing with PBS, the cells were incubated with the fluorescent secondary antibody, Alexa Fluor 488-labeled goat anti-mouse IgG (1:400, Thermo Fisher Scientific Inc.; cat. no. A-11001) or Alexa Fluor 594-labeled goat anti-rabbit IgG (1:400, Thermo Fisher Scientific Inc.; cat. no. A-11012) at 25 °C for 2 h. Nuclei were stained with DAPI (Southern Biotech, Birmingham, AL, USA), and all the images were obtained under a fluorescence microscope (BX53, Olympus, Tokyo, Japan), an Olympus DP74 camera, and the cellSens Standard software at magnification x200. The immunofluorescence intensities for Beclin 1 and p53 were evaluated in six different areas of each slide using ImageJ software (ver. 1.53e), and the immunofluorescence intensity ratio was calculated in comparison to that of the nuclear staining of DAPI, as a reference for the adjustment of cell number. Autophagosome (LC3B dots)-positive cells were detected in six different areas of each slide and counted by two researchers, including one histopathologist. The proportion of the number of autophagosome-positive cells to the total number of cells was evaluated for the adjustment of cell number. To confirm autophagosomes, images were obtained under a confocal laser scanning microscope (FV1000, Olympus), an Olympus DP74 camera, and cellSens Standard software at magnification x1200.

2.4. Establishment of a nude mouse model bearing NPC cell xenograft

Four-week-old male nude mice (BALB/c athymic nu/nu mice) were purchased from Japan SLC, Inc. (Hamamatsu, Japan). All animal protocols were approved by the Committee of the Animal Center of Mie University, Mie, Japan (approval no. 26–19-sai3). The mice were acclimated for 1 week with tap water and a pelleted diet *ad libitum* before the start of the experiment. They were housed under controlled conditions of humidity (50 ± 10 %), light (12/12 h light and dark cycle), and temperature (22 ± 2 °C).

1.5×10^6 HK1-EBV cells were subcutaneously transplanted into the right flank of nude mice (n = 12, 5-week-old, body weight; average 16.3 g, standard deviation [SD], 0.6 g). Five days after transplantation, when the diameter of the tumors reached 2–3 mm, the mice were randomly divided into two groups (n = 6 per group): i) control group, administered distilled water *ad libitum*; ii) taurine-treated group, administered 0.5 % (w/v) taurine (Nacalai Tesque Inc.) dissolved in distilled water *ad libitum* (day 1). The sample size was determined according to the method reported by Charan and Kantharia (Charan and Kantharia, 2013) using tumor weight as the primary outcome. Tumor size was measured with a caliper (model 530–312; range 0–150 mm; Mitutoyo, Kawasaki, Japan) every three days after randomization. Based on the method described by Tu et al. (Tu et al., 2018), tumor volumes were calculated as follows:

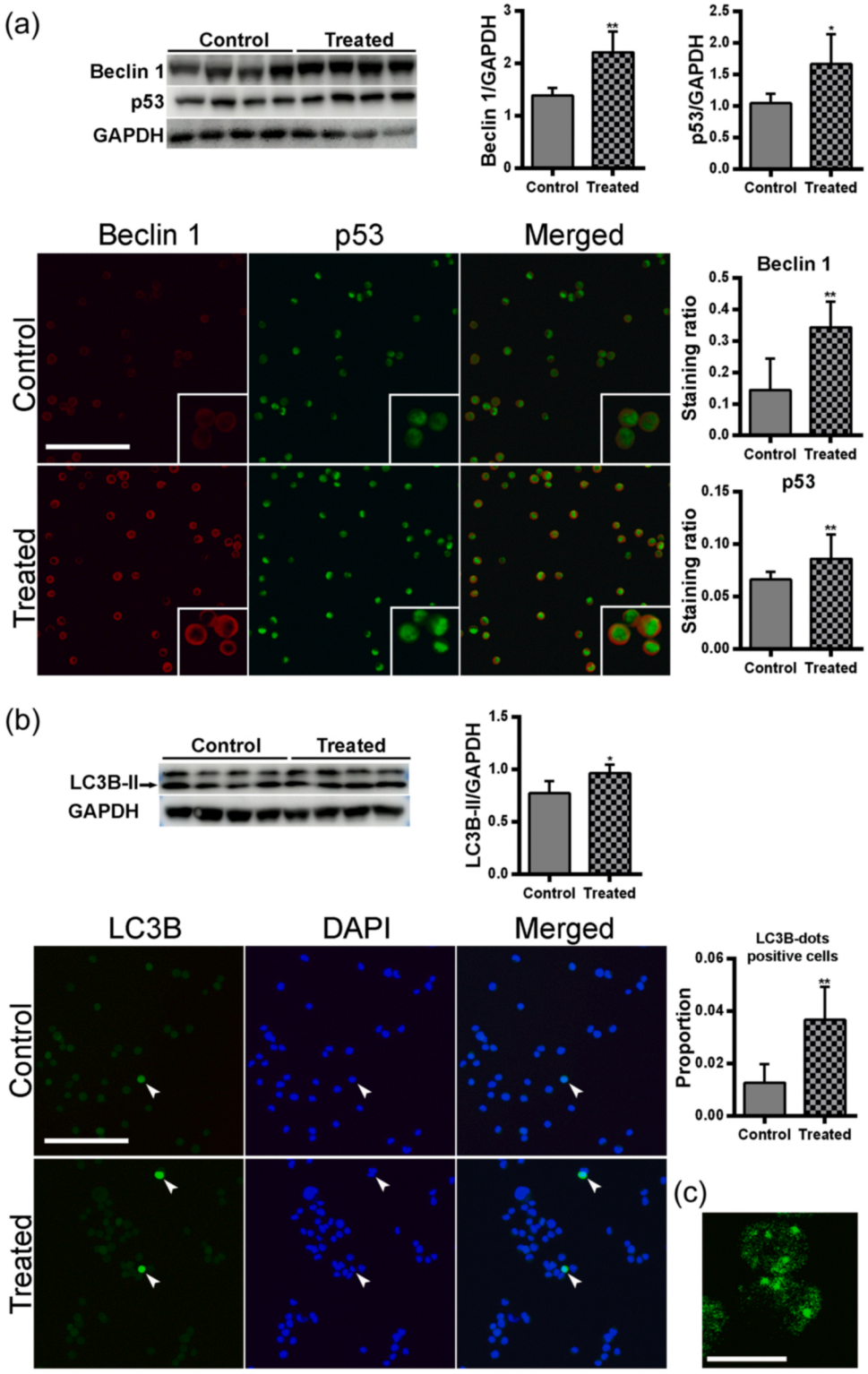

Fig. 1. Effects of taurine on NPC cells *in vitro*. HK1-EBV cells were treated with taurine at 32 mM for 48 h. (a) Western blot analyses and immunofluorescence staining of cells against Beclin 1 and p53. Double immunofluorescence staining of the cells shows the co-expression of Beclin 1 and p53 in the control cells and taurine-treated cells. Images in the insets are enlarged pictures. For immunofluorescence analyses, graphs represent the average and SD (bar) of immunofluorescence intensity ratio between target and DAPI. Scale bars, 100 μm. (b) Western blot analyses and immunofluorescence staining of cells against LC3B. Arrowheads indicate LC3B-dots positive cells. For immunofluorescence analyses, graph represents the average and SD (bar) of the proportion of the number of autophagosome-positive cells to the total number of cells. Scale bars, 100 μm. All experiments of Western blot were performed in quadruplicate. GAPDH was used as a loading control. Graphs represent the average and SD (bar) of the band intensity ratio between target and GAPDH. *, $p < 0.05$; **, $p < 0.01$ between control and taurine-treated cells. (c) Autophagosomes in the LC3B-dots positive cells observed by laser confocal microscopy. Scale bar, 10 μm.

tumor volume (mm^3) = $1/2 \times a \times b^2$ (where a is the longer arm and b is the shorter arm). The mice were euthanized on day 13 after randomization and the tumors were resected, photographed, and weighed.

2.5. IHC analyses

Immediately after photographing and weighing, the tumor tissue samples were fixed with 4 % (v/v) formaldehyde in phosphate-buffered saline for one day. Following dehydration and paraffin infiltration, samples were embedded in paraffin blocks. Then, the blocks were sectioned to 5 μm thickness using Leica Microsystem (Wetzler, Germany) using routine protocols and heated at 40 °C for 48 h. Paraffin-embedded sections were deparaffinized in xylene and rehydrated in serial alcohol solutions. Antigen retrieval was performed in 5 % (w/v) urea by boiling the samples for 5 min in a microwave oven (500 W). Following epitope retrieval, endogenous peroxidases were inactivated

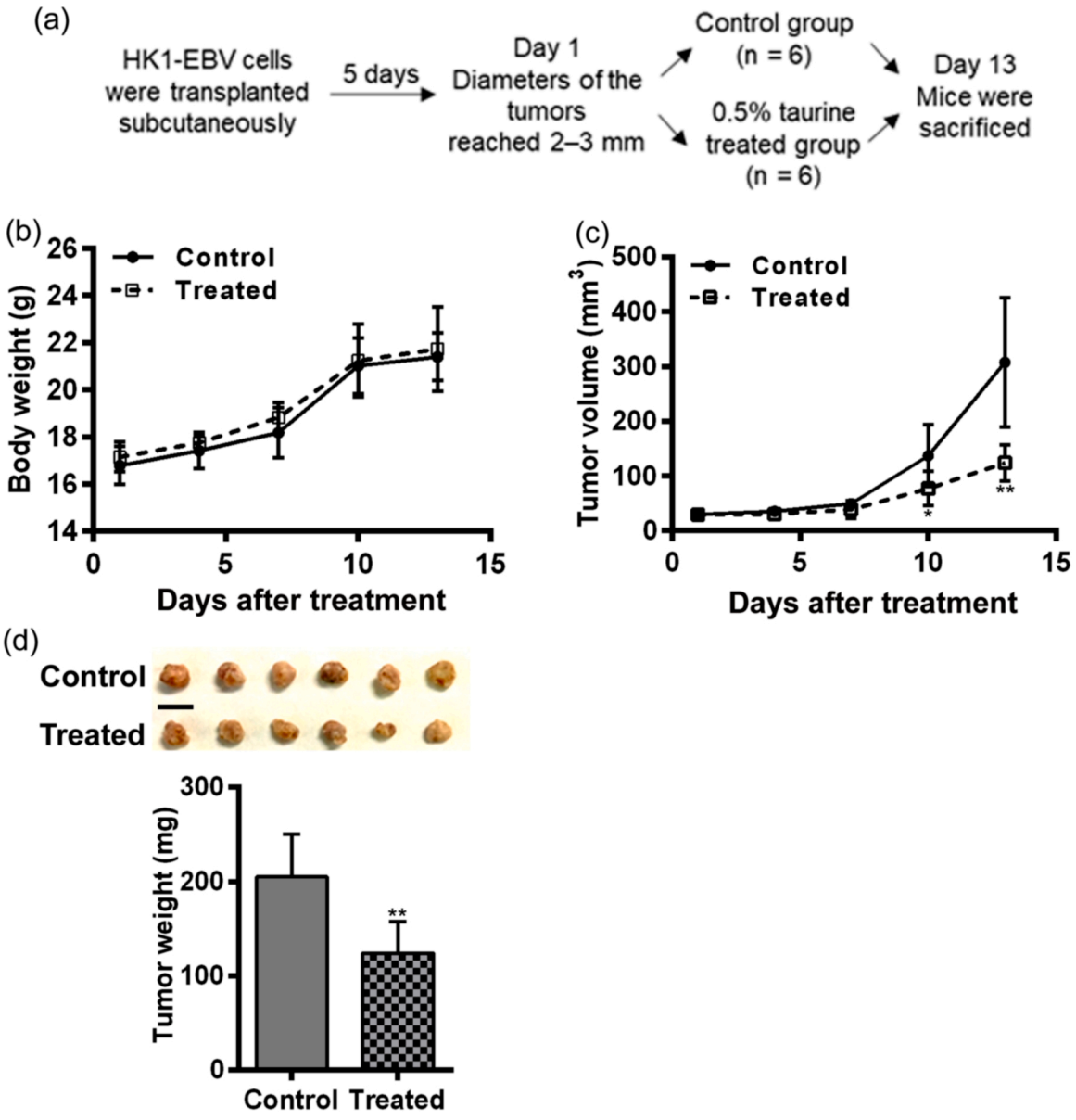

Fig. 2. Effects of taurine on tumor growth in nude mouse xenografts. (a) Experimental protocol. (b) Body weight of mice. (c) Growth curve of tumors (volume) in nude mice bearing HK1-EBV cell xenografts. (d) Resected tumors and the tumor weight of the xenografts of HK1-EBV cells from nude mice drinking water (control) and 0.5 % taurine (treated). Scale bar, 10 mm. Graphs represent the average and SD (bar). *, $p < 0.05$; **, $p < 0.01$ between control and taurine-treated groups.

using 1 % (v/v) H_2O_2 at 25 °C for 15 min. The sections were blocked with 1 % (w/v) skimmed milk (Becton Dickinson) for 20 min. Sections were then incubated with following primary antibodies at 25 °C overnight: macrophage migration inhibitory factor (MIF) (rabbit IgG, kind gift from Dr. Takuma Kato, Mie University, as previously reported (Ohkawara et al., 2002), 1:200), taurine transporter (TAUT) (mouse IgG1, Santa Cruz Biotechnology Inc.; cat. no. sc-393036, 1:200), taurine (rabbit IgG, 1:150) produced by Ma et al., as previously reported (Ma et al., 1994), cleaved caspase-3 (rabbit IgG, Cell Signaling Technology Inc.; cat. no. 9661s, 1:200), Bcl-xL (rabbit IgG; Cell Signaling Technology Inc., cat. no. 2764s, 1:200), p53 (mouse IgG2a; Merck, cat. no. OP43, 1:200), phosphatase and tensin homolog (PTEN) (rabbit IgG, Cell Signaling Technology Inc.; cat. no. 9188s, 1:200), LC3B (mouse IgG2b; Cell Signaling Technology Inc., cat. no. 83506s, 1:200), Beclin 1 (rabbit IgG, Abcam plc; cat. no. ab62557, 1:200), transcription factor EB (TFEB) (rabbit IgG, Cell Signaling Technology Inc.; cat. no. 37785s, 1:200), phospho- (p-) extracellular signal-related kinase 1 and 2 (ERK1/2) (rabbit IgG, Cell Signaling Technology Inc.; cat. no. 4370s, 1:200) and p-4E-BP1 (rabbit IgG, Cell Signaling Technology Inc., cat. no. 2855s, 1:200). After washing with PBS, they were incubated with biotinylated secondary antibodies (Vector Laboratories, Burlingame, CA, USA) at 25 °C for 1 h. The immunocomplexes were visualized using a peroxidase stain DAB kit (Nacalai Tesque, Inc.), according to the manufacturer's instructions. Nuclei were counterstained with hematoxylin. To evaluate the immunohistochemical specificity, we set a negative control section by staining without the primary antibody for each IHC scoring. All images were obtained under a microscope (BX53, Olympus), an Olympus DP74 camera, and cellSens Standard software at a magnification of x200.

França et al. (França et al., 2013) reported that head and neck squamous carcinoma cells tested positive for MIF and consistently expressed MIF, independent of their location. Hence, we defined the areas positive for MIF as the tumor parenchyma of the tumor tissue samples. For localization of the tumor cells, neighboring sections for hematoxylin and eosin staining were used to confirm the MIF-positive area (Supplementary Figure S1). The MIF-positive area coincident

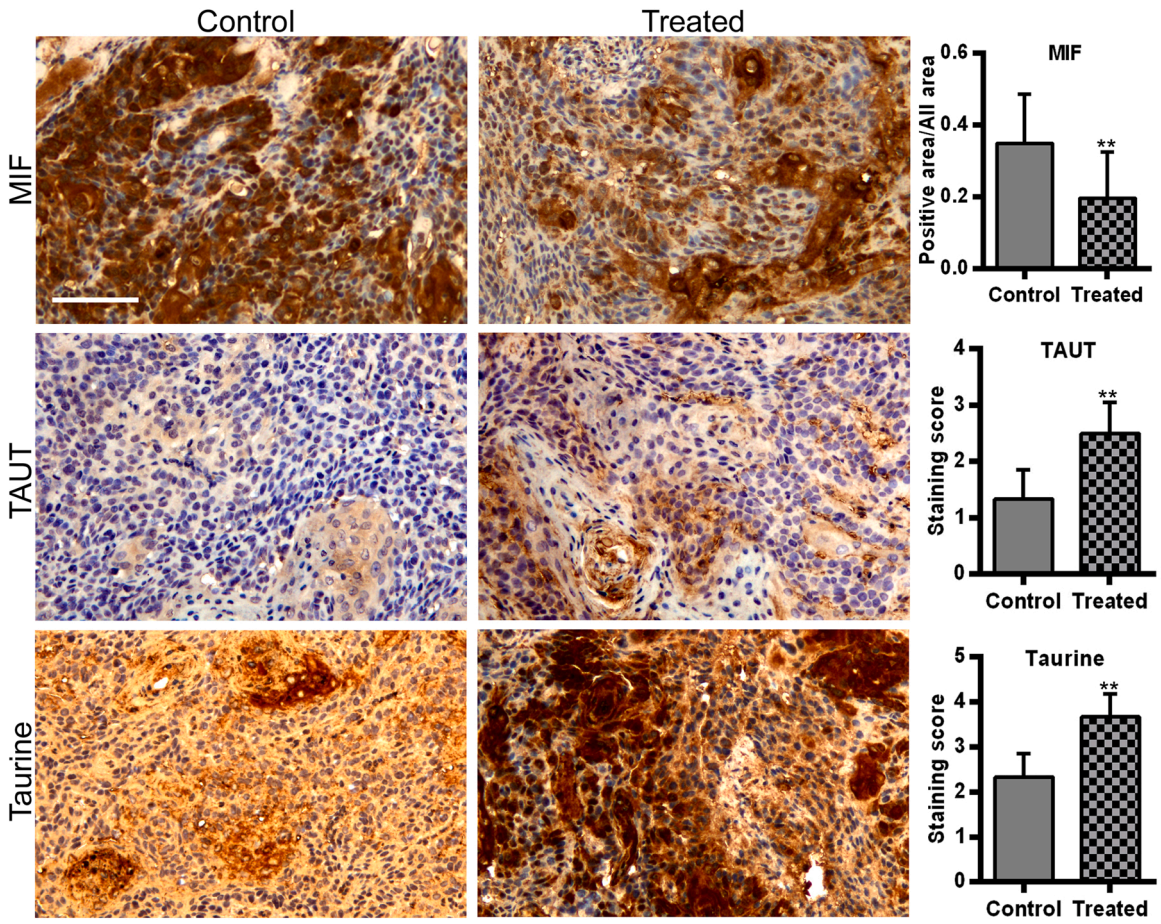

Fig. 3. Effects of taurine on MIF-positive area, TAUT, and taurine in xenograft tumor tissues. Immunoreactivities of MIF, TAUT, and taurine were assessed using an avidin-biotin kit with peroxidase-based detection (brown). Nuclei were counterstained with hematoxylin. Graph represents the average proportion and SD (bar) of the MIF-positive area to the total area. Graphs represent the average score and SD (bar) for TAUT and taurine. *, $p < 0.05$; **, $p < 0.01$ between control and taurine-treated groups. Scale bar, 100 μm.

with the tumor parenchyma in the sections was determined by two investigators, including one histopathologist, and measured using ImageJ software (ver. 1.53e), using a freehand selection tool.

Semi-quantitative analyses were performed by grading the staining intensity with an IHC score of 0–4 by two investigators, including one histopathologist, as follows: no staining (0), weak staining (1 +), moderate staining (2 +), strong staining (3 +), and very strong staining (4 +) in sections with IHC staining of TAUT, taurine, cleaved caspase-3, Bcl-xL, p53, PTEN, LC3B, Beclin 1, TFEB, p-ERK1/2, and p-4E-BP1, by focusing on the areas assessed as cancer nests. Each antigen was stained at least thrice in each group. Images were obtained from three fields in each section for analysis.

2.6. Statistical analyses

Comparisons of data between the two groups were performed by Student's t-test using GraphPad Prism 6 software (GraphPad Software Inc., San Diego, CA, USA). Statistical significance was set at $P < 0.05$.

3. Results

3.1. Taurine upregulates Beclin 1 and p53 expressions in HK1-EBV cells with the upregulation of autophagy in vitro

To assess the effect of taurine on Beclin 1 and p53 expressions in NPC cells *in vitro*, the expression of Beclin 1 and p53 was investigated by Western blotting and ICC analyses. Western blot analyses showed that treating HK1-EBV cells with taurine induced a significant increase in the Beclin 1 and p53 levels (Fig. 1a, upper panel; Beclin 1, $p = 0.0084$; p53, $p = 0.0475$). ICC analyses also showed a significant increase in the levels of Beclin 1 (red) and p53 (green) in the taurine-treated cells (merged, Fig. 1a, lower panel; Beclin 1, $p < 0.0001$; p53, $p = 0.0003$). Furthermore, treatment with taurine significantly increased the levels of LC3B-II (Fig. 1b, upper panel; $p = 0.0360$) and the proportion of autophagosome (LC3B dots)-positive cells (Fig. 1b, lower panel; $p = 0.0021$). Laser confocal microscopy confirmed the presence of autophagosomes in NPC cells (Fig. 1c).

3.2. Taurine suppresses tumor growth of NPC cells in a nude mouse xenograft model

NPC cell xenografts were induced in nude mice by subcutaneous transplantation of HK1-EBV cells, followed by drinking distilled water or 0.5 % taurine *ad libitum* (Fig. 2a). All mice were alive at the end of the experiment. There was no significant difference in mouse body weight between the control group and the treated group at any time point (Fig. 2b). The tumor volume in the mice increased gradually, but the taurine treatment caused slower tumor growth than that in the control group (Fig. 2c, day 10, $p = 0.0482$; day 13, $p = 0.0045$). At the end of the experiment (day 13), the tumors were resected, and the average tumor weight was significantly lower in the taurine-treated group than that in the control group (Fig. 2d, $p = 0.0054$).

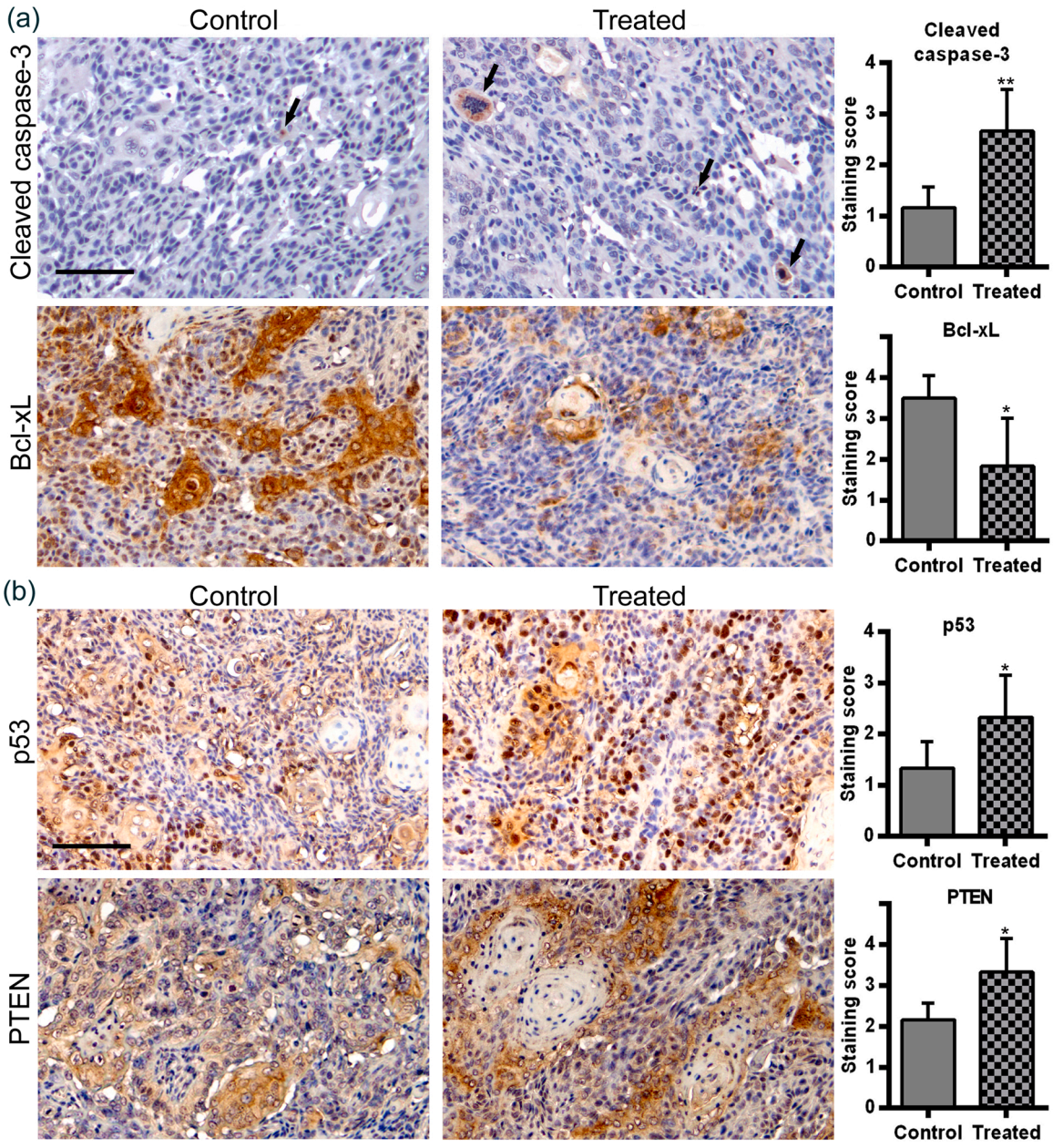

Fig. 4. Effects of taurine on apoptosis-related molecules in xenograft tumor tissues. Immunohistochemical staining of (a) cleaved caspase-3 and Bcl-xL, (b) p53, and PTEN. Graphs represent the average score and SD (bar) for cleaved caspase-3, Bcl-xL, p53, and PTEN. Cleaved caspase-3 positive cells are indicated by black arrows. *, $p < 0.05$; **, $p < 0.01$ between control and taurine-treated groups. Scale bars, 100 μm.

3.3. MIF-positive areas are decreased and Taurine and TAUT levels are increased in tumor xenografts of nude mice by taurine administration

IHC analysis (Fig. 3) revealed a notable decrease in MIF-positive areas, designated as NPC cancer nests, in the taurine-treated group compared with that in the control group ($p = 0.0015$). Furthermore, we found that TAUT was significantly upregulated ($p = 0.0035$), and the staining intensity for taurine was markedly increased ($p < 0.0001$) in the tumor tissues of the taurine-treated group compared to that in the control group (Fig. 3).

3.4. Taurine affects apoptosis-related molecules in xenograft tumor tissues

The staining scores for cleaved caspase-3 were significantly higher in tumor tissues from the taurine-treated group (Fig. 4a, $p = 0.0024$). The antiapoptotic molecule Bcl-xL was significantly downregulated in the taurine-treated group compared with that in the control group (Fig. 4a, $p = 0.0101$). The present study also showed significantly higher expression levels of p53 ($p = 0.0296$) and PTEN ($p = 0.0107$) in xenograft tumor tissues of taurine-treated nude mice (Fig. 4b).

3.5. Taurine upregulates autophagy-associated proteins with upregulation of TFEB, a master autophagy regulator, and downregulation of ERK1/2 in xenograft tumor tissues

We performed semiquantitative analyses of autophagy-associated molecules. LC3B, an autophagy marker, is required for the expansion and completion of autophagic membranes (Barth et al., 2010), and Beclin 1 is an important autophagy component (Yue et al., 2003). The expression levels of LC3B ($p = 0.0346$) and Beclin 1 ($p = 0.0165$) were significantly increased in xenograft tumor tissues of the taurine-treated

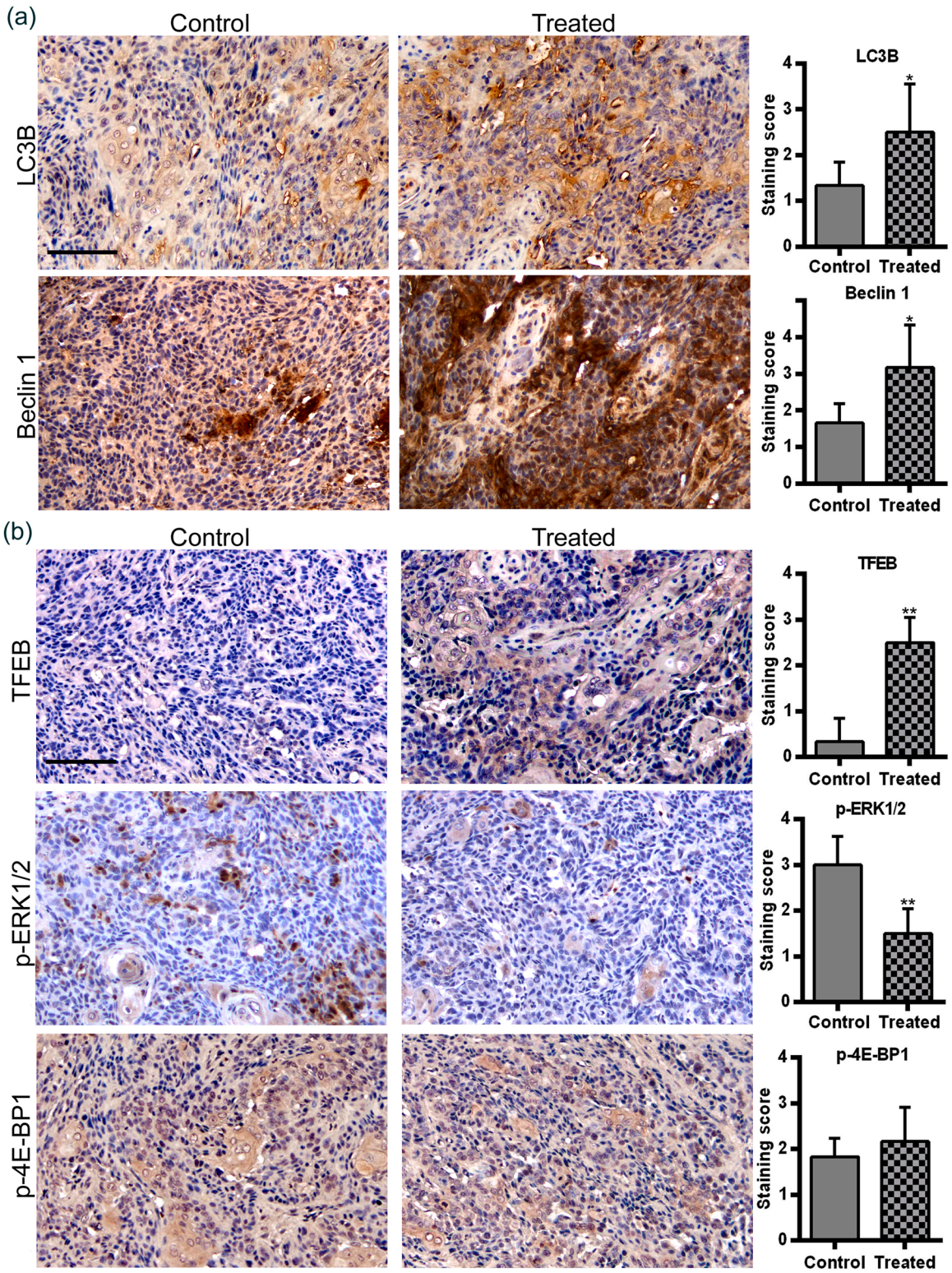

Fig. 5. Effects of taurine on autophagy-related proteins and modulators in xenograft tumor tissues. Immunohistochemical staining of (a) autophagy-related proteins LC3B and Beclin 1, and (b) modulators of autophagy, TFEB, p-ERK1/2, and p-4E-BP1. Graphs represent the average score and SD (bar) for LC3B, Beclin 1, TFEB, p-ERK1/2, and p-4E-BP1. * , $p < 0.05$; * *, $p < 0.01$ between control and taurine-treated groups. Scale bars, 100 μm.

group (Fig. 5a).

TFEB is a master autophagy regulator and activates Beclin 1 and LC3B (Bahrami et al., 2020). The TFEB expression level ($p < 0.0001$) was also significantly increased in xenograft tumor tissues of the taurine-treated group (Fig. 5b). TFEB is negatively regulated by several kinase pathways including ERK1/2 and the mechanistic target of rapamycin protein kinase complex 1 (mTORC1) (Settembre et al., 2011). Hence, we investigated the levels of phosphorylated substrates of the kinase pathway (p-ERK1/2, and a substrate of mTORC1, p-4E-BP1). The p-ERK1/2 level significantly decreased ($p = 0.0014$), whereas there was

no significant difference in the p-4E-BP1 expression levels ($p = 0.3628$, Fig. 5b). Likewise, Western blot analyses showed that treating NPC cells with taurine downregulated the p-ERK1/2 expression level without affecting p-4E-BP1 *in vitro* (Supplementary Figure S2).

4. Discussion

In this *in vitro* study, taurine upregulated both Beclin 1 and p53 in NPC cells and concurrently upregulated autophagy. Additionally, the present *in vivo* study demonstrated higher levels of both Beclin 1 and p53 in the taurine-treated group, with higher LC3B and cleaved caspase-3 staining scores. The antitumor effects of taurine on apoptosis have been reported in some types of cancer cells, such as glioblastoma, lung cancer, and colon cancer *in vitro* (Surarak et al., 2021; Tu et al., 2018; Zhang et al., 2014), and the authors suggested the involvement of p53. A recent report (Kaneko et al., 2018) showed that taurine treatment activates autophagy in adipocytes. Although the role of autophagy in anticancer effects remains controversial, Beclin 1, which is crucial for phagophore formation initiation in the autophagy process, has been previously characterized as a tumor suppressor in mammalian cells (Yue et al., 2003). Furthermore, Liu et al. reported that Beclin 1 upregulates p53 and functions as a tumor suppressor (Liu et al., 2011). Our results and the literature suggest that taurine may induce autophagy and apoptosis in cancer cells, including NPC, *via* Beclin 1 and p53 upregulation.

In our *in vivo* study, we set the optimal concentration of 0.5 % taurine in drinking water (approximately 40 mM), which was similar to the effective dose (32 mM) *in vitro*. Taurine is now used as a preventive or therapeutic agent for the recurrence of stroke-like episodes in mitochondrial diseases, mitochondrial myopathy, encephalopathy, lactic acidosis, and stroke-like episodes (MELAS), by oral supplementation (12 g/day) from the results of clinical trials (Ohsawa et al., 2019). This therapeutic dose of taurine is approximately 0.2–0.3 g/kg/day. In this study, 0.5 % taurine in drinking water was estimated as 0.4 g/kg/day. Therefore, the dose used in the animal experiments was relevant to the therapeutic dose. The present *in vivo* study confirmed the antitumor effect of taurine on the tumor growth of NPC cell xenografts in a nude mouse model. These observations suggest that taurine can be ingested *via* drinking and can affect NPC xenograft tumors in nude mice. This result is supported by our previous study, which showed that taurine dose-dependently inhibited cell proliferation in NPC cells *in vitro* (He et al., 2018). Interestingly, in xenograft tumor tissues treated with taurine, the expression of TAUT and the amount of taurine were significantly increased. Zhang et al. reported elevated intracellular taurine levels and upregulation of TAUT expression in cardiac tissues of taurine-treated acute myocardial ischemia model rats (Zhang et al., 2013). To the best of our knowledge, this is the first report to show that taurine treatment increases TAUT expression and results in higher taurine levels in tumor tissues *in vivo*. This may contribute to the anticancer effect of taurine at this dose, which is considered therapeutically relevant.

The present *in vivo* study demonstrated that taurine upregulated PTEN and p53, along with an increase in cleaved caspase-3 and a decrease in the antiapoptotic protein Bcl-xL levels in tumor tissues with a reduction in tumor growth. Our previous *in vitro* study also showed that taurine induced apoptosis in NPC cells *via* the PTEN and p53 signaling pathways (He et al., 2018). These results suggest that taurine induces apoptosis in transplanted NPC cells *in vivo,* similar to previous observations in NPC cells *in vitro*. Interestingly, taurine reduced the viability and induced apoptosis of NPC cells, but did not affect normal human nasopharyngeal epithelial NP460 cells (He et al., 2018). The present study showed no adverse effects of taurine on nude mice based on changes in body weight. These results suggest that taurine could serve as a potential chemopreventive agent.

We first demonstrated that taurine upregulated autophagy-associated proteins in NPC tissues, as evidenced by increased LC3B and Beclin 1 levels, and further showed that taurine downregulated the p-ERK1/2 expression level and upregulated the TFEB expression level without affecting the mTORC1 substrate, p-4E-BP1. We also confirmed that taurine treatment under the same condition downregulated the p-ERK1/2 expression level without affecting p-4E-BP1 in NPC cells *in vitro* by Western blot analyses. These results are consistent with those reported by Kaneko et al. (Kaneko et al., 2018), who showed that taurine activated autophagy *via* TFEB upregulation and downregulation of the mitogen-activated protein kinase (MAPK)/ERK signaling pathway without affecting the mTORC1 signaling pathway in the adipocyte cell line 3T3-L1. From these results and the literature, we envision that increased taurine in the tumor tissues may upregulate the autophagic regulator Beclin 1, which may increase p53 levels, leading to the induction of autophagy and apoptosis in the tumor tissues. However, IHC analyses were insufficient to manipulate the pathways underlying taurine-induced anticancer mechanisms. Further studies are needed to clarify the pathways involved in the induction of autophagy and apoptosis in cancer.

5. Conclusions

The present study demonstrated that taurine induced upregulation of Beclin 1 and p53 in NPC cells *in vitro* and *in vivo,* and suppressed tumor growth in nude mouse xenografts of NPC cells. Taurine may have an anticancer effect *via* upregulation of Beclin1 and p53, with the induction of autophagy and apoptosis. Taurine may be a promising chemopreventive and/or therapeutic agent for NPC.

Funding

This work was supported in part by Japan Society for the Promotion of Science, JSPS KAKENHI (grant number JP19K22757 [MM]).

CRediT authorship contribution statement

Conceptualization, I.T. and M.M.; Methodology, N.M. and K.N.; Investigation, M.O., F.H., N.M.; Writing – original draft, M.O.; Writing – review & editing, H.K., S.O., I.T., and M.M.; Supervision, I.T. and M.M.; Project administration; I.T. and M.M. All authors read and approved the final manuscript.

Conflict of interest

The authors declare that they have no conflicts of interest.

Data Availability

Data will be made available on request.

Acknowledgments

We are deeply grateful to Professor Sai-Wah Tsao at Hong Kong University and Dr. Takuma Kato at Mie University for their kind contribution to the human NPC cell line (HK1-EBV) and primary antibody against MIF, respectively.

Appendix A. Supporting information

Supplementary data associated with this article can be found in the online version at doi:10.1016/j.acthis.2022.151978.

References

Bahrami, A., Bianconi, V., Pirro, M., Orafai, H.M., Sahebkar, A., 2020. The role of TFEB in tumor cell autophagy: diagnostic and therapeutic opportunities. Life Sci. 244, 117341 https://doi.org/10.1016/j.lfs.2020.117341.

Barth, S., Glick, D., Macleod, K.F., 2010. Autophagy: assays and artifacts. J. Pathol. 221 (2), 117–124. https://doi.org/10.1002/path.2694.

Chang, E.T., Ye, W., Zeng, Y.X., Adami, H.O., 2021. The evolving epidemiology of nasopharyngeal carcinoma. Cancer Epidemiol. Biomark. Prev. 30 (6), 1035–1047. https://doi.org/10.1158/1055-9965.epi-20-1702.

Charan, J., Kantharia, N.D., 2013. How to calculate sample size in animal studies. ? J. Pharmacol. Pharmacother. 4 (4), 303–306. https://doi.org/10.4103/0976-500x.119726.

Chen, Y.P., Chan, A.T.C., Le, Q.T., Blanchard, P., Sun, Y., Ma, J., 2019. Nasopharyngeal carcinoma. Lancet 394 (10192), 64–80. https://doi.org/10.1016/s0140-6736(19)30956-0.

França, C.M., Batista, A.C., Borra, R.C., Ventiades-Flores, J.A., Mendonça, E.F., Deana, A. M., Mesquita-Ferrari, R.A., de Natali Caly, D., de Mello Rode, S., Faria, M.R., 2013. Macrophage migration inhibitory factor and oral cancer. J. Oral. Pathol. Med. 42 (5), 368–373. https://doi.org/10.1111/jop.12011.

He, F., Ma, N., Midorikawa, K., Hiraku, Y., Oikawa, S., Zhang, Z., Huang, G., Takeuchi, K., Murata, M., 2018. Taurine exhibits an apoptosis-inducing effect on human nasopharyngeal carcinoma cells through PTEN/Akt pathways in vitro. Amino Acids 50 (12), 1749–1758. https://doi.org/10.1007/s00726-018-2651-2.

He, F., Ma, N., Midorikawa, K., Hiraku, Y., Oikawa, S., Mo, Y., Zhang, Z., Takeuchi, K., Murata, M., 2019. Anti-cancer mechanisms of taurine in human nasopharyngeal carcinoma cells. Adv. Exp. Med. Biol. 1155, 533–541. https://doi.org/10.1007/978-981-13-8023-5_49.

Huang, D.P., Ho, J.H., Poon, Y.F., Chew, E.C., Saw, D., Lui, M., Li, C.L., Mak, L.S., Lai, S. H., Lau, W.H., 1980. Establishment of a cell line (NPC/HK1) from a differentiated squamous carcinoma of the nasopharynx. Int. J. Cancer 26 (2), 127–132. https://doi.org/10.1002/ijc.2910260202.

Ibrahim, H.M., Abdel Ghaffar, F.R., El-Elaimy, I.A., Gouida, M.S., Abd El Latif, H.M., 2018. Antitumor and immune-modulatory efficacy of dual-treatment based on levamisole and/or taurine in Ehrlich ascites carcinoma-bearing mice. Biomed. Pharmacother. 106, 43–49. https://doi.org/10.1016/j.biopha.2018.06.113.

Kabeya, Y., Mizushima, N., Ueno, T., Yamamoto, A., Kirisako, T., Noda, T., Kominami, E., Ohsumi, Y., Yoshimori, T., 2000. LC3, a mammalian homologue of yeast Apg8p, is localized in autophagosome membranes after processing. EMBO J. 19 (21), 5720–5728. https://doi.org/10.1093/emboj/19.21.5720.

Kaneko, H., Kobayashi, M., Mizunoe, Y., Yoshida, M., Yasukawa, H., Hoshino, S., Itagawa, R., Furuichi, T., Okita, N., Sudo, Y., Imae, M., Higami, Y., 2018. Taurine is an amino acid with the ability to activate autophagy in adipocytes. Amino Acids 50 (5), 527–535. https://doi.org/10.1007/s00726-018-2550-6.

Kim, C., Cha, Y.N., 2014. Taurine chloramine produced from taurine under inflammation provides anti-inflammatory and cytoprotective effects. Amino Acids 46 (1), 89–100. https://doi.org/10.1007/s00726-013-1545-6.

Kim, Y.S., Kim, E.K., Hwang, J.W., Kim, W.S., Shin, W.B., Natarajan, S.B., Moon, S.H., Jeon, B.T., Park, P.J., 2017. Taurine attenuates doxorubicin-induced toxicity on B16F10 Cells. Adv. Exp. Med. Biol. 975 (Pt 2), 1179–1190. https://doi.org/10.1007/978-94-024-1079-2_94.

Lambert, I.H., 2004. Regulation of the cellular content of the organic osmolyte taurine in mammalian cells. Neurochem. Res. 29 (1), 27–63. https://doi.org/10.1023/b:nere.0000010433.08577.96.

Lambert, I.H., Hoffmann, E.K., Pedersen, S.F., 2008. Cell volume regulation: physiology and pathophysiology. Acta Physiol. (Oxf.) 194 (4), 255–282. https://doi.org/10.1111/j.1748-1716.2008.01910.x.

Lang, P.A., Warskulat, U., Heller-Stilb, B., Huang, D.Y., Grenz, A., Myssina, S., Duszenko, M., Lang, F., Häussinger, D., Vallon, V., Wieder, T., 2003. Blunted apoptosis of erythrocytes from taurine transporter deficient mice. Cell. Physiol. Biochem. 13 (6), 337–346. https://doi.org/10.1159/000075121.

Leung, S.F., Zee, B., Ma, B.B., Hui, E.P., Mo, F., Lai, M., Chan, K.C., Chan, L.Y., Kwan, W. H., Lo, Y.M., Chan, A.T., 2006. Plasma Epstein-Barr viral deoxyribonucleic acid quantitation complements tumor-node-metastasis staging prognostication in nasopharyngeal carcinoma. J. Clin. Oncol. 24 (34), 5414–5418. https://doi.org/10.1200/jco.2006.07.7982.

Levy, J.M.M., Towers, C.G., Thorburn, A., 2017. Targeting autophagy in cancer. Nat. Rev. Cancer 17 (9), 528–542. https://doi.org/10.1038/nrc.2017.53.

Liu, J., Xia, H., Kim, M., Xu, L., Li, Y., Zhang, L., Cai, Y., Norberg, H.V., Zhang, T., Furuya, T., Jin, M., Zhu, Z., Wang, H., Yu, J., Li, Y., Hao, Y., Choi, A., Ke, H., Ma, D., Yuan, J., 2011. Beclin1 controls the levels of p53 by regulating the deubiquitination activity of USP10 and USP13. Cell 147 (1), 223–234. https://doi.org/10.1016/j.cell.2011.08.037.

Lo, A.K., Lo, K.W., Tsao, S.W., Wong, H.L., Hui, J.W., To, K.F., Hayward, D.S., Chui, Y.L., Lau, Y.L., Takada, K., Huang, D.P., 2006. Epstein-Barr virus infection alters cellular signal cascades in human nasopharyngeal epithelial cells. Neoplasia 8 (3), 173–180. https://doi.org/10.1593/neo.05625.

Ma, N., Aoki, E., Semba, R., 1994. An immunohistochemical study of aspartate, glutamate, and taurine in rat kidney. J. Histochem. Cytochem 42 (5), 621–626. https://doi.org/10.1177/42.5.7908911.

Ma, N., He, F., Kawanokuchi, J., Wang, G., Yamashita, T., 2022. Taurine and its anticancer functions: in vivo and in vitro study. Adv. Exp. Med. Biol. 1370, 121–128. https://doi.org/10.1007/978-3-030-93337-1_11.

Maher, S.G., Condron, C.E., Bouchier-Hayes, D.J., Toomey, D.M., 2005. Taurine attenuates CD3/interleukin-2-induced T cell apoptosis in an in vitro model of activation-induced cell death (AICD). Clin. Exp. Immunol. 139 (2), 279–286. https://doi.org/10.1111/j.1365-2249.2005.02694.x.

Ohkawara, T., Nishihira, J., Takeda, H., Hige, S., Kato, M., Sugiyama, T., Iwanaga, T., Nakamura, H., Mizue, Y., Asaka, M., 2002. Amelioration of dextran sulfate sodium-induced colitis by anti-macrophage migration inhibitory factor antibody in mice. Gastroenterology 123 (1), 256–270. https://doi.org/10.1053/gast.2002.34236.

Ohsawa, Y., Hagiwara, H., Nishimatsu, S.I., Hirakawa, A., Kamimura, N., Ohtsubo, H., Fukai, Y., Murakami, T., Koga, Y., Goto, Y.I., Ohta, S., Sunada, Y., 2019. Taurine supplementation for prevention of stroke-like episodes in MELAS: a multicentre, open-label, 52-week phase III trial. J. Neurol. Neurosurg. Psychiatry 90 (5), 529–536. https://doi.org/10.1136/jnnp-2018-317964.

Schuller-Levis, G.B., Park, E., 2003. Taurine: new implications for an old amino acid. FEMS Microbiol. Lett. 226 (2), 195–202. https://doi.org/10.1016/s0378-1097(03)00611-6.

Settembre, C., Di Malta, C., Polito, V.A., Garcia Arencibia, M., Vetrini, F., Erdin, S., Erdin, S.U., Huynh, T., Medina, D., Colella, P., Sardiello, M., Rubinsztein, D.C., Ballabio, A., 2011. TFEB links autophagy to lysosomal biogenesis. Science 332 (6036), 1429–1433. https://doi.org/10.1126/science.1204592.

Surarak, T., Chantree, P., Sangpairoj, K., 2021. Synergistic effects of taurine and temozolomide via cell proliferation inhibition and apoptotic induction on U-251 MG human glioblastoma cells. Asian Pac. J. Cancer Prev. 22 (12), 4001–4009. https://doi.org/10.31557/apjcp.2021.22.12.4001.

Tu, S., Zhang, X.L., Wan, H.F., Xia, Y.Q., Liu, Z.Q., Yang, X.H., Wan, F.S., 2018. Effect of taurine on cell proliferation and apoptosis human lung cancer A549 cells. Oncol. Lett. 15 (4), 5473–5480. https://doi.org/10.3892/ol.2018.8036.

Wang, G., Ma, N., He, F., Kawanishi, S., Kobayashi, H., Oikawa, S., Murata, M., 2020. Taurine attenuates carcinogenicity in ulcerative colitis-colorectal cancer mouse model. Oxid. Med. Cell. Longev. 2020, 7935917. https://doi.org/10.1155/2020/7935917.

Yamori, Y., Taguchi, T., Hamada, A., Kunimasa, K., Mori, H., Mori, M., 2010. Taurine in health and diseases: consistent evidence from experimental and epidemiological studies. J. Biomed. Sci. 17 (Suppl 1), S6. https://doi.org/10.1186/1423-0127-17-s1-s6.

Yue, Z., Jin, S., Yang, C., Levine, A.J., Heintz, N., 2003. Beclin 1, an autophagy gene essential for early embryonic development, is a haploinsufficient tumor suppressor. Proc. Natl. Acad. Sci. U. S. A. 100 (25), 15077–15082. https://doi.org/10.1073/pnas.2436255100.

Zhang, X., Tu, S., Wang, Y., Xu, B., Wan, F., 2014. Mechanism of taurine-induced apoptosis in human colon cancer cells. Acta Biochim Biophys. Sin. (Shanghai) 46 (4), 261–272. https://doi.org/10.1093/abbs/gmu004.

Zhang, Y., Yang, L., Yang, Y.J., Liu, X.Y., Jia, J.G., Qian, J.Y., Wang, K.Q., Zuo, J., Ge, J. B., 2013. Low-dose taurine upregulates taurine transporter expression in acute myocardial ischemia. Int. J. Mol. Med. 31 (4), 817–824. https://doi.org/10.3892/ijmm.2013.1264.

Methods

Supplementary Figure S1. To confirm the tumor cells, and exclude nonspecific staining in necrotic tissues, we compared MIF-positive area and hematoxylin and eosin staining of the neighboring section. The MIF-positive area coincident with tumor parenchyma in the sections were determined by two investigators, including one histopathologist, and measured using ImageJ software (ver. 1.53e) by freehand selection tool, as described in “2.5. IHC analyses”.

Supplementary Figure S2. Western blot analyses were performed, using primary antibodies; phospho-extracellular signal-related kinase 1 and 2 (ERK1/2) (rabbit IgG, Cell Signaling Technology Inc.; cat. no. 4370s, 1:1000) and phospho-4E-BP1 (rabbit IgG, Cell Signaling Technology Inc.; cat. no. 2855s, 1:1000), as described in “2.2. Western blot analyses”.

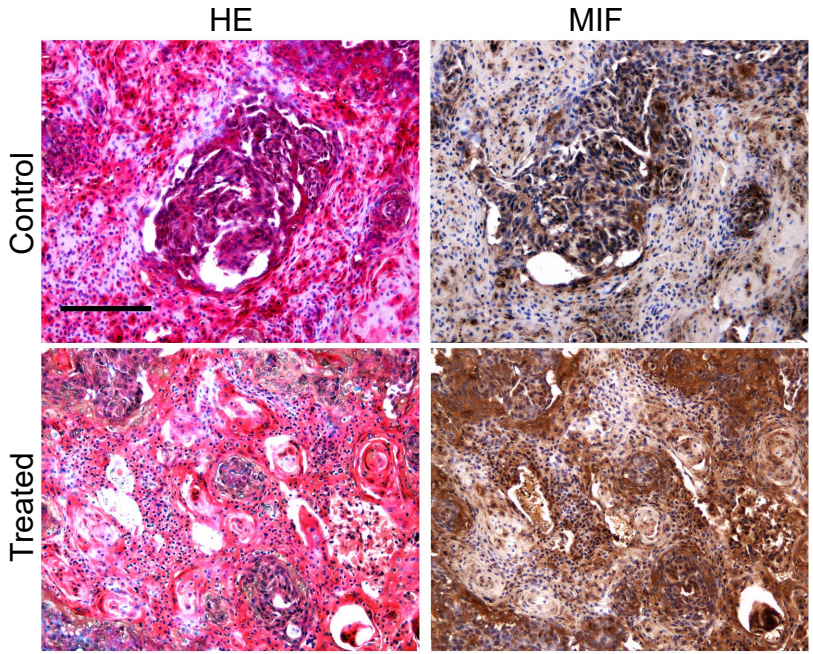

Supplementary Figure S1. Hematoxylin and eosin staining and immunohistochemical staining by MIF using neighboring sections. Scale bar, 100 μm.

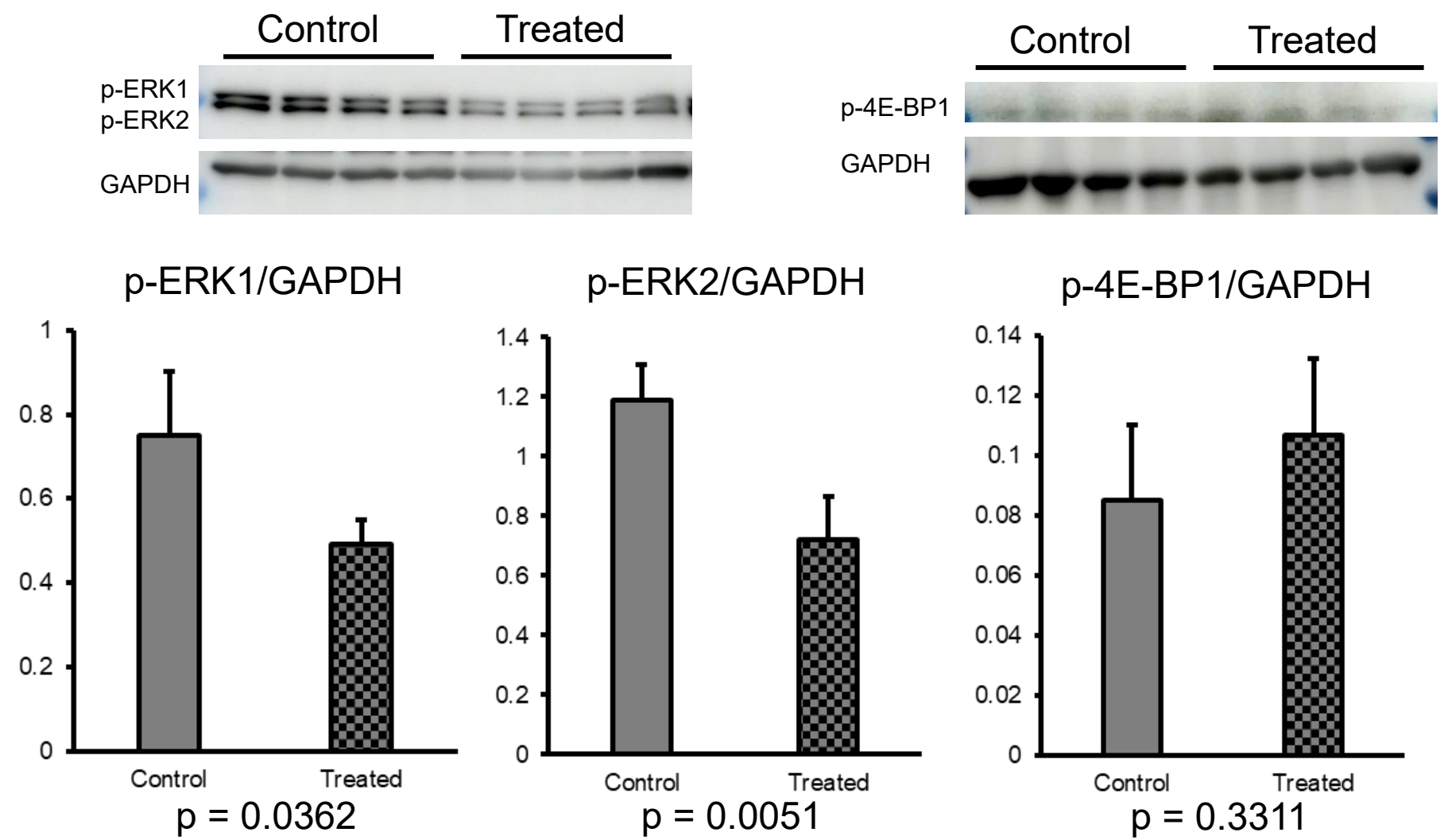

Supplementary figure S2. Effects of taurine on phospho-ERK1/2 in NPC cells. Western blot against phospho-ERK1/2 and phospho-4E-BP1. HK1-EBV cells were treated with 32 mM taurine for 48 h. Western blot was performed in quadruplicate. GAPDH was used as a loading control. Graphs represent the average and SD (bar) of the band intensity ratio between target and GAPDH.